

Review of Color Features and CNN's Raw Arecanut Image Classification

Satheesha K M

Research Scholar, Electronics and Communication Department, Srinivas Institute of Engineering and Technology, Srinivas University, Mangalore

Lecturer, Electronics and Communication Department Karnataka Govt Polytechnic Mangalore

ABSTRACT

One of the significant economic crops in India is the arecanut (*Areca catechu* L.). There are many computer-based technologies for other types of crops, however there isn't a computer vision-based sophisticated technology for classifying an arecanut's grade, variety, and illnesses. This research proposes a review on unique way for categorizing arecanut into two groups based on colour. Three phases make up the suggested methodology: segmentation, masking, and classification. Color space is transformed from the RGB picture. The picture is effectively segmented into arecanuts using three sigma control limits. Three sigma control limits are used to represent the arecanut colour space, which covers the majority of variance in the arecanut's color components. Effective segmentation of the arecanut is accomplished by using the upper and lower boundaries of the colour components. The segmented section of the arecanuts is classified by its red and green colour components. An experimental finding demonstrates the effectiveness of the suggested strategy.

Keywords - Segmentation; Classification; Arecanut, Deep Neural Networks, U-Net, Mask R-CNN, Feature Pyramid Network.

I. INTRODUCTION

One common and significant crop for certain Taiwanese is the areca nut. In Taiwan, the annual output value of areca nuts exceeds NTD 100,000 million. Although chewing areca nuts can lead to oral cancer [1], they are frequently referred to as Taiwanese gum in Taiwan. Arecas are often grown on mountain slopes with moderate air movement. Areca nuts are frequently contaminated by a variety of diseases, such as bacteria, viruses, fungus, or dangerous insects. Areca nut surface damage will result in a decrease in price. It has been sorted thus far in Taiwan using conventional labour. Farmers' revenue is continually impacted by the labor expense and sorting time.

Several methods for classifying fruits, foods, and seeds have been proposed. The literature [3] on the use of machine vision for aquatic food applications is divided into sections on composition analysis, measurement and evaluation of size and volume, measurement of parameter estimates, quantification of the colour of the outside or meat of aquatic foods, and defect detection during quality assessment. The following steps are included in a reliable algorithm for separating food from background images when using colour images: I compute a high contrast grey value image from the

best linear combination of the RGB colour components; (ii) estimating a global threshold using a statistical approach; and (iii) performing morphological operations to fill in any potential gaps in the segmented binary image [2]. Physical attributes, such as the main, intermediate, and minor mass and volume of three mutually perpendicular axes, were measured in order to get the necessary parameters for the detection method and calibration pictures. An estimation of the watermelon's mass/volume is made by computing the area from the 2D picture [3]. It was suggested to classify tomatoes using image processing [4]. Short, medium-sized, and tall kiwifruits were identified using an aspect ratio, while flattened fruits were identified using an ellipsoid ratio as a second parameter [5]. Measurements were made of the cantaloupe fruit's geometrical features and several physical traits, including length, major diameter, minor diameter, mass, volume, and density [6]. determining the mean colour intensity to distinguish between the various shades or levels of oil palm maturity fruits is proposed.

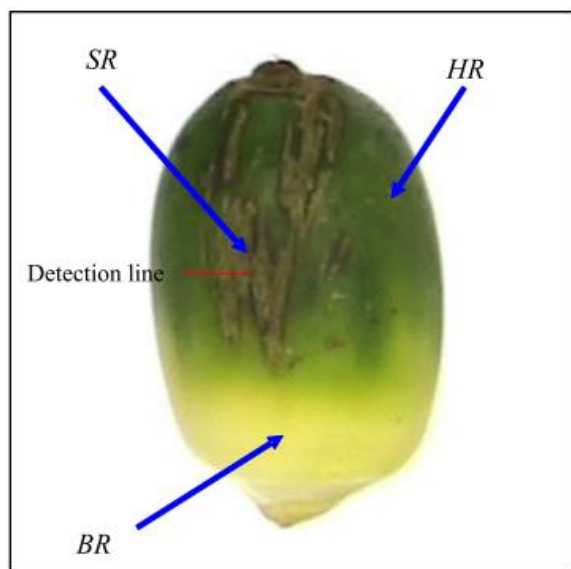


Figure No. 1 – An Arecanut Image

Using a Neural Network Classifier, a unique technique is used to grade oranges into three quality bands based on their surface properties, such as size, shape, surface colouring, and fault marks [8]. For each picture, fuzzy the mamdani inference and adaptive fuzzy neural network (anfis) techniques were employed to classify the tomato [9]. A technique for image processing was created to assess the stone fruit's colour [10]. Simply measuring the object's radius at a given location and integrating along the length yields the approximate papaya volume. Finally, using the volume data, papaya weights are estimated [13]. Color representation, colour quantization, and classification algorithm are three crucial aspects of the colour pixel classification method to skin segmentation that need more investigation [14]. created and put into use a prototype back propagation neural network classifier date fruit grading and sorting system based on a set of external quality features [15]. Using a colour histogram approach, an automated grading system for *Jatropha curcas* was developed to separate the fruits' levels of maturity based on colour intensity [8].

II. LITERATURE SURVEY

To the best of our knowledge, no effort has been made to classify arecanuts using an image processing technique, even though classification of fruits, flowers, seeds, etc. has been done. Four varieties of arecanuts are considered in this essay. Those are gorublu, api, bette, and mine. To

categorization, the nuts are divided into just two categories: boiling nuts (BN), which include api, bette, and minne, and non-boiling nuts, which include gorublu (NBN). In our method, the colour component of arecanuts may be used to classify them. We performed a survey at roughly 15 places and found the following findings:

- The hue of all the gorublu arecanuts will be reddish yellow (Belongs to NBN class).
- The whole bette, api, and minne are green. (Is a member of the BN class).
- The BN class also includes nuts that are transitioning from bette to gorublu and contain 25% green pigment.

Inherently ill-posed and domain dependent, general-purpose segmentation is highly difficult. Effective object representation is another difficulty. Most of the segmentation methods now in use focus on a binary classification method, such as crops vs. backgrounds. Background removal is a crucial phase that must be carried out correctly to prevent misclassification. When it comes to arecanut segmentation, very little effort is done. The analysis of various segmentation strategies for other comparable commodities has a direct bearing on our issue.

Crop recognition and segmentation are difficult since the crop's colour and sharpness vary in an outside field as the lighting changes. Furthermore, when the illumination changes, the intricacy is greatly heightened by shadows and interreflection. Since immature crop is mostly green in colour and mimics the backdrop vegetation, segmenting it is significantly more challenging. Additionally, within a single crop bunch, there will be a minor difference in the colours of the various components, which makes crop segmentation more difficult. For instance, an arecanut bunch has nuts that are green and yellow in hue. The use of colour in segmentation methods also has its advantages. The most effective visual signal used to identify one thing from another is colour. Second, in situations with persistent illumination, colour mostly remains stable when an object's size, direction, and blockage change [4]. The two primary categories of color-based techniques are pixel-based and region-based approaches. In most cases, RGB colour space is used to describe images that digital cameras record in the electromagnetic spectrum. RGB colour is also seen by humans. With the use of linear or non-

linear transformations, additional colour spaces can be produced from RGB space. To overcome concerns with light variance during picture capture, other colour spaces are employed. ExGRcolour model provides better results for the green vegetation segmentation in the field compared to other colour models for the photos that were obtained in varied environmental circumstances with varying backdrops, according to a thorough analysis on several pixel-based techniques.

Segmentation, masking, and classification are the three processes of a paper that proposes a two-class categorization of arecanuts based on color [12]. The red and green arecanut segment's components are what are being evaluated here. Another study [3] investigating texture characteristics for categorization. First, the arecanut is segmented using global based threshold and Otsu techniques, and then it is classified using mean around and grey level co-occurrence matrix (GLCM) features. Another study uses support vector machines (SVMs) and colour characteristics to categorize arecanuts into boiling and non-boiling nuts utilizing three sigma control limits on colour features utilized for segmentation [11].

The data set made available by **R. Dhanesha et al.** [13] has been utilized to train and test the performance of the networks to evaluate the techniques. Because features are automatically extracted from the photos to provide the best representation of the inputs, the usage of deep neural networks enhances segmentation accuracy. Results were contrasted with cutting-edge methods using well-known measures. More information on the U-Net and Mask R-CNN architectures utilized for arecanut bunch segmentation will be provided in the next sections.

Image processing is a potent technology that is frequently used to find agricultural items. To evaluate the quality of photographs, colour, geometric, and texture aspects are frequently utilised. Using a neural network with input nodes for texture characteristics such contrast, diagonal moment, energy, entropy, homogeneity, second diagonal moment, and uniformity, **Park et al.** [2] suggested a technique of content-based picture categorization. Nine textural characteristics were employed by **Hsieh et al.** [3] to train a neural network to identify the head cabbage seedlings' development stage.

Segmentation techniques based on machine learning (ML) have grown in popularity. Gray-scale picture gradients are used to identify edges in a method to segment ripe grape bunches, and the Hough transform is subsequently used to identify circles [12]. Three grape cluster recognition techniques employing shape matching, C5.0 decision tree training using patches of foliage and grape regions, and distribution of edges between the foliage and grape clusters were given in [13]. Most segmentation approaches focus on using certain characteristics of the target item to be segmented, such as colour, texture, and form [14]. These manually created characteristics do not provide effective segmentation. The focus of researchers has shifted to deep learning-based techniques like convolutional neural networks (CNN).

In the literature, all studies have divided the arecanut without the husk into two categories: those that have been boiled and those that have not. The current study, however, focuses on dividing the raw arecanut (arecanut with husk) into four categories.

III. PROPOSED SYSTEM

Segmentation, feature extraction, and classification are the three phases of the suggested model. Using the K-means clustering approach, the collected photos were initially divided into two areas that represented the background and foreground. The segmentation is done to get rid of the shadow that was cast when taking the picture. Following that, moment characteristics and the colour histogram are derived from segmented pictures. We employed the supervised K-NN classifier for classification. As a result, after extracting the features for the classifier, we must train it before evaluating it by comparing test photos to the trained ones. The class that the train image belongs to will be indicated on the test image if it matches.

Based on the elements of colour, arecanuts are categorised in this work. Color space is transformed from the RGB picture. To establish the ucl (upper control limit) and lcl (lower control limit) of the colours using equations (1), (2), (3), and (4), the red and blue colour components of arecanut objects were manually cut from the photos.

$$ucl_{cb} = \mu_{cb} + 3\sigma_{cb} \quad - 1$$

$$lcl_{cb} = \mu_{cb} - 3\sigma_{cb} \quad - 2$$

$$ucl_{cr} = \mu_{cr} + 3\sigma_{cr} \quad - 3$$

$$lcl_{cr} = \mu_{cr} + 3\sigma_{cr} \quad - 4$$

Where:

$$\mu_{cb} = \frac{1}{M \times N} \sum_{i=1}^M \sum_{j=1}^N CB(i, j) \quad - 5$$

$$\mu_{cr} = \frac{1}{M \times N} \sum_{i=1}^M \sum_{j=1}^N CR(i, j) \quad - 6$$

And Standard Deviation can be calculated using the formula:

$$\sigma_{cb} = \sqrt{\frac{1}{M \times N} \sum_{i=1}^M \sum_{j=1}^N CR((i, j) - \mu_{cr})} \quad - 7$$

$$\sigma_{cr} = \sqrt{\frac{1}{M \times N} \sum_{i=1}^M \sum_{j=1}^N CR((i, j) - \mu_{cb})} \quad - 8$$

IV. DATA SET USED

With more than 170 satellites already in orbit, the PlanetScope small satellite constellation outperforms all existing satellites in terms of resolution (3–4 m), frequency (daily), and worldwide coverage [15]. We chose a clean, cloudless, and high-quality PlanetScope satellite image taken on March 21 for the present study. The utilised PlanetScope picture is an orthographic data product (3B) that has undergone orthorectification, atmospheric correction, sensor, and radiometric calibration. There are four spectral bands in the blue, green, red, and near-infrared sections of the satellite picture, which has a spatial resolution of 3 m. The PlanetScope satellite's parameters. Farmland, woodland, impermeable surface (urban and rural areas; industrial and mining; water conservancy construction; and transportation land), water (rivers, lakes, ponds, etc.), and arecanut grove are the main land use/cover categories in the study region. The primary aspects of the research area's visual interpretation characteristics are listed in Table 2. On March 19–21, 2019, GPS-enabled field surveys were used to collect ground sample data. The field's

covering area should be larger than 10 m by 10 m. The field boundaries were then established based on the location of the survey locations using Google Earth Pro (version 7.3.2.5776). Finally, 850 field polygon samples in total were identified.

On the 10th and 11th of February 2013, just before the Hyperion imagery needed to create the spectral library was purchased, reflectance data of arecanut foliage of various age groups was obtained. A grid-wise data collecting approach was chosen, and 100 m² of grid were used to acquire a typical spectrum. For typical plots, measurements of tree top reflectance were made. Using an ASD portable Spectroradiometer Field Spec® with a wavelength range of 325-1075 nm and a resolution of 1 nm, leaf samples were obtained from remote farms. The representative spectral signatures were derived by comparing and averaging a set of 20 samples. To create a vector layer of typical farms with a range of ages and varied crops, about 80 farms were surveyed using GPS technology. The built-in vector layer helps the training site-based supervised classification process.

V. MATERIAL AND METHODS

Image acquisition system: It was created a machine vision system to take pictures of areca nuts. This system consists of a personal computer, a GigE CCD (coupled-charge device) colour camera (DFK-31AG03, Imaging Source Inc.), and a zoom lens (Intel Pentium 4 processor 2.4 GHz). To get RGB colour pictures of 640 480 pixels, the applications were coupled to the Open-Source Computer Vision Library (OpenCV 1.0, Intel Corporation). For image capture, a CCD camera with a 4600 lx and F4.0 opening was used (iris diaphragm). Images were kept in tagged image file (TIF) format on a PC's hard disc. With the aid of Microsoft Visual C++ 6.0, image processing was carried out.

5. 1: Feature Extraction

Segmenting the full picture of the areca nut is a crucial step once the areca nut's characteristics have been retrieved. The thresholding, hole-filling, closing, and opening processes separate the areca nut picture into its component parts [13]. First, the areca nut's principal axis must be determined. By assuming that $f(x_i, y_i)$, where $i = 1, 2, \dots, m$, and the total number of pixels is m , represents the binary representation of an areca nut. The centroid can be

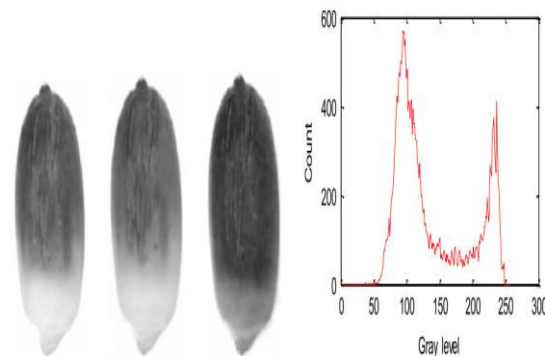
calculated using the formula $\bar{x} = \sum_{i=1}^M \frac{x_i}{m}$ and $\bar{y} = \sum_{y=1}^N \frac{y_i}{n}$. The covariance matrix's orthogonal eigenvectors are computed. Eigenvectors are used to calculate the geometric features of the entire areca nut, including the principal axis length (Lp), secondary axis length (Ls), the centroid, axis number (Lp/Ls), area (A), perimeter (P), compactness ($4A/P^2$), and color features (Rm, Gm, and Bm, or the mean grey level of areca nut on the R, G, and B bands). Second, these geometrical and visual characteristics will be used in the categorization of areca nuts.

5.2: Spot Region Detection:

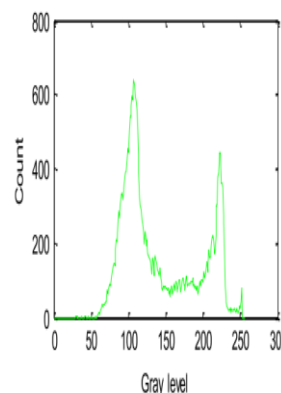
According to Fig. 2, the look of an areca nut has three distinct sections: healthy regions (HR), base regions (BR), and spot regions (SR). Once the damaged areca nut has been located, it is crucial to effectively segment SR. The thresholding approach makes it challenging to discern between SR and HR, though. For instance, the grey level histogram cannot be used to determine whether to extract SR using the thresholding decision rule. The threshold values (T) 160, 150, and 80 are employed in Fig. 2 to separately segment the SR on the red (R), green (G), and blue (B) bands (Fig. 2(a)-(c)). Fig. 2(g)-(i) The segmentation outcomes were displayed (i). As a result, a fresh approach must be suggested for the study's SR segmentation of areca nuts.

This experiment came before another one. To discover the grey levels of the areca nut picture, a detection line with scanning resolution in a pixel was first used. As shown in Fig. 3, there are various grey level distribution patterns in HR, SR, and BR. According to Fig. 3, the curves of grey level on the R and G bands are similar in the HR area (a). Even a few instances of R, G, and B curves intersecting (at points C1, C2, and C3) happened. The distinct areas of grey level are undoubtedly on SR. Additionally, as demonstrated in Fig. 3, distinct grey levels were visible on BR (b). To resolve the overlapping instances, the areca nut picture was secondly handled with the smoothing operator [18] (as seen in Fig. 4). With a detection line, as shown in Fig. 5, it is possible to acquire the distributions of grey level on the SR, HR, and BR. The sites C1, C2, and C3 on the SR and HR illustrated in Fig. 5 were acquired after a smooth procedure, thus there are obvious discrepancies. As a result, SR, HR, and

BR may be distinguished based on the variance in grey levels between the R, G, and B bands.



(a) Red gray image. (b) Green gray image. (c) Blue gray image. (d) Histogram for red gray image.



(e) Histogram for green gray image. (f) Histogram for blue gray image.



(g) Binary image on red band (T = 160). (h) Binary image on green band (T = 150). (i) Binary image on blue band (T = 80).

5.3 :Classification

Analyses of geometric and colour aspects have been used extensively in the categorization process. In this study, areca nut quality was categorised using geometric and colour criteria. To categorise the quality of areca nuts, six geometric parameters (namely, the primary axis length, secondary axis, axis number, area, perimeter, and compactness), three colour features (namely, the mean grey level on the R, G, and B bands: Rmean, Gmean, and Bmean), and SR area were used. Every time a pattern recognition method is required, the artificial neural network (ANN) has found several uses. In this investigation, areca nuts were divided into excellent, good, and terrible classes using a back propagation neural network [14] (BPNN, as illustrated in Fig. 6). Three layers make up the BPNN classifier: an input layer, a hidden layer, and an output layer. The input layer comprises 10 nodes that are associated to the SR region, three colour features, and the previously stated six geometric characteristics. It generalises the input characteristics between 0 and 1. Nodes from three categories—Excellent (E), Good (G), and Bad—make up the output layer (B). Initially, the formula below was used to determine the quantity of nodes n_h in the hidden layer.

$$n_h = [(n_i + n_o)/2] + (n_p)^{0.5}$$

where n_p is the number of input patterns in the training set, n_i is the number of input nodes, n_o is the number of output nodes, and n_o is the number of output nodes. Finding a connection in a pattern that was created by the characteristics of each is the goal of the learning process of areca nut.

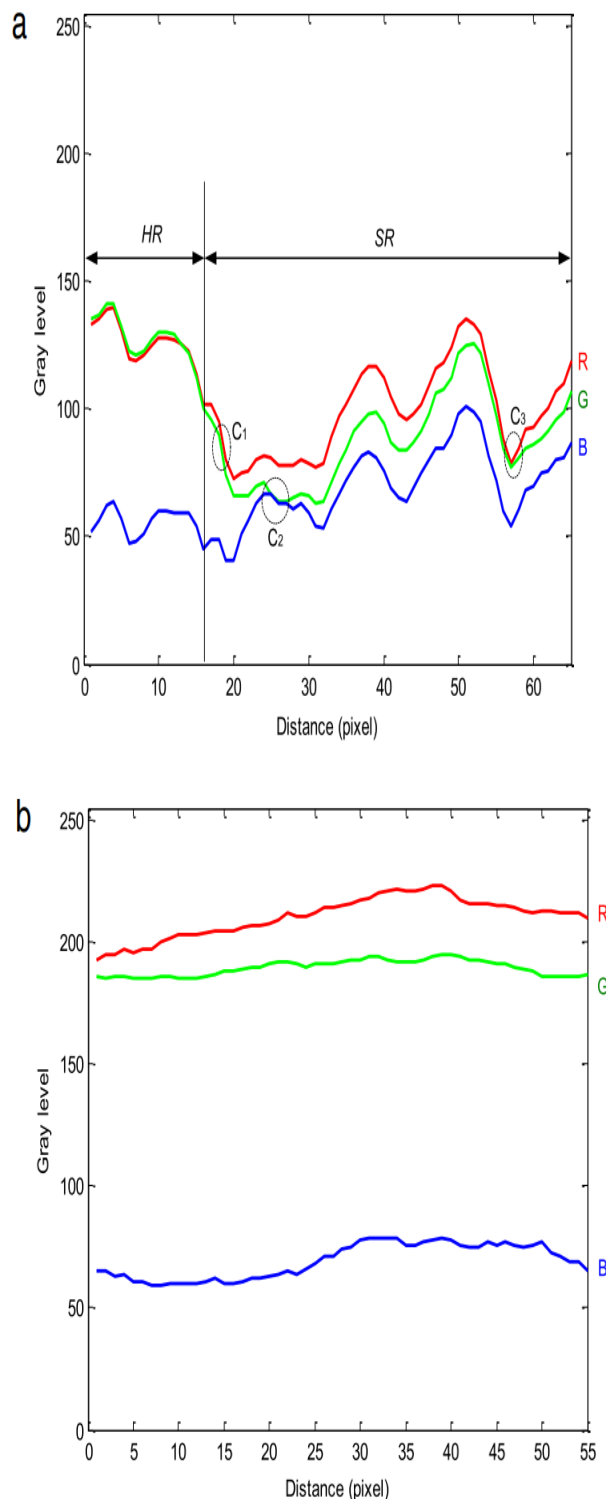


Figure No. 3 - The distribution of gray level for an original areca nut image. (a) HR and SR. (b) BR.

After training, the weights are adjusted until the error convergence threshold is met, which is 0.1. The error message is shown by

$$E(t) = \sum_{p=1}^3 e_p(t) = \sum_{p=1}^3 |d_p(t) - y_p(t)|$$

where $y_p(t)$ is the signal produced by neuron p at iteration t , and $d_p(t)$ is the expected response for neuron p ($p = 1-3$). The DL algorithm, the BPNN classifier, and image processing methods were used to create the algorithm for the identification and classification of areca nuts. Following is a description of the algorithm:

Step 1: Estimate the areca nut's three hues and six geometrical aspects.

Step 2: SR area estimate and segmentation.

Step 3: Create and evaluate the BPNN classifier to categorize the areca nut quality.

VI. RESULT AND DISCUSSION

For this study, the most widely used commercial arecanut cultivar is considered. The database includes 629 photos from 15 distinct places, 71 of which are used for testing while the rest 558 are used for training. Images with a resolution of 3000x4000 pixels were captured with a Canon digital color camera (Power Shot A1100IS). All the photos were taken outside in daylight with a white background, about filling the camera's field of view. For suitable computing performance, image resolution was reduced to 150x200 pixels. The suggested approach effectively divides different arecanuts into two groups, BN and NBN, as shown in table 1, including api, bette, mine, and gorublu. The dirty and broken nuts are to blame for the categorization error.

Class	Sample of Testing	Misclassification	Success Rate
BN	412	5	99.01
NBN	193	5	98.12

Table No. 1 - Examples of experimental categorization outcomes using supervised learning with unidentified samples.

VII. CONCLUSION

To separate the arecanuts from the picture in this study, we employed control limits. Only the red and green colour components, which are ordinarily subdued in the segmented region, are employed to categorise the arecanuts. Using three sigma deviations from the mean, the upper and

lower control limits of the blue chroma and red chroma colour components are established. The arecanut areas can be divided using these regulatory limits. The segmented area of the arecanut is further classified using its red and blue colour components. The effectiveness of the suggested strategy was demonstrated by experimental data. This approach may be used to classify various objects, such as fruits, seeds, flowers, and other things where sorting and grading are typically handled by professionals.

REFERENCES

- [1]. P.S Hiremath and AjitDanti, Detection of multiple faces in an image using skin color information and Lines-of-Separability face model. International Journal of Pattern recognition and Artificial Intelligence, World scientific Publisher; 2016, Vol. 20(1), pp. 39-61.
- [2]. Meftah Salem M Alfatni, Abdul Rashid Mohamed Shariff, Helmi ZuhaidiMohdShafri, Osama M Ben saaed and Omar M Eshanta. Oil Palm Fruit Bunch Grading System Using Red, Green and Blue Digital Number. Journal of Applied Sciences; 2018, 8(8):1444-1452.
- [3]. SalmatRiyadi, Mohd. Marzuki Mustafa, Aini Hussain and Azman Hamza, Papaya fruit grading based on size using image analysis. Proceedings of the International Conference on Electrical Engineering and Informatics Institute Teknologi Bandung, Indonesia; 2017, 17-19
- [4]. J.A. Marchant, C.M. Onyango, Comparison of a Bayesian classifier with a multilayer feed-forward neural network using the example of plant/weed/soildiscrimination, Computers and Electronics in Agriculture 39 (2003) 3–22.
- [5]. K.Y. Huang, T.C. Lin, Estimating the geometric characteristics of Phalaenopsis orchid during big plant stage with machine vision, Journal of Agricultural Machinery 9 (2) (2020) 13–26 (in Chinese).
- [6]. L. Fauset, Fundamentals of Neural Networks: Architectures, Algorithms, and Applications, Prentice-Hall, Upper Saddle River, New Jersey, 2021
- [7]. ShrinivasaNaika C.L R Dhanesha. and Y. Kantharaj. Segmentation of arecanut bunches usingycgr color model. 1st International Conferenceon Advances in Information Technology (ICAIT), pages 50–53, 2019.

- [8]. Kaiming He et al. Mask r-cnn. *Computer Vision and Pattern Recognition*, 2018.
- [9]. Toni P. Saarela Landy and Michael S. Combination of texture and color cues in visual segmentation. *Vision Research*, pages 56–67, 2019.
- [10]. S K Niranjana Siddesha S and V N Manjunath Aradhya. A study of different color segmentation techniques for crop bunch in arecanut. *Handbook of Research on Advanced Hybrid Intelligent Techniques and Applications*.
- [11]. J.A. Marchant, C.M. Onyango, Comparison of a Bayesian classifier with a multilayer feed-forward neural network using the example of plant/weed/soil discrimination, *Computers and Electronics in Agriculture* 39 (2003) 3–22.
- [12]. Hassan Sadrnia, Ali Rajabipour, Ali Jafary, Arzhang Javadi and Younes Mostofi. Classification and Analysis of Fruit Shapes in Long Type Watermelon Using Image Processing. *International Journal of Agriculture & Biology*; 2007, 1560–8530, 09–1–68–70.
- [13]. Rasmus Houborg Matthew F. McCabe and Arko Lucieer. High-resolution sensing for precision agriculture: from earth-observing satellites to unmanned aerial vehicles. *Remote Sensing for Agriculture, Ecosystems and Hydrology*.
- [14]. T.N. Prakash B.J. Rajkumar and B.N. Pradeepa Babu. Indigenous technical knowledge (itk) and farmers willingness to practice- an economic study of arecanut peeling machines in Karnataka. *International Research Journal of Agricultural Economics and Statistics*, 6(2):307–316, 2019.
- [15]. Y. Wang Z. H. Yu X. F. Zhang C. N. Li X. D. Bai, Z. G. Cao. Crop segmentation from images by morphology modeling in the $CIE\ L^*a^*b^*$ color space. *Computers and Electronics in Agriculture*, 99:21–34, 2020.